

Density dependence of the nuclear symmetry energy: a microscopic perspective

Isaac Vidaña, Constança Providência

*Centro de Física Computacional, Department of Physics,
University of Coimbra, 3004-516 Coimbra, Portugal*

Artur Polls

*Departament d'Estructura i Constituents de la Matèria and Institut de Ciències del Cosmos,
Universitat de Barcelona, Avda. Diagonal 647, E-08028 Barcelona, Spain*

Arnau Rios

*Faculty of Engineering and Physical Sciences,
Department of Physics, University of Surrey,
Guildford, Surrey GU2 7XH, United Kingdom and
Kavli Institute for Theoretical Physics China (CAS),
100190 Beijing, People's Republic of China*

Abstract

We perform a systematic analysis of the density dependence of the nuclear symmetry energy within the microscopic Brueckner–Hartree–Fock (BHF) approach using the realistic Argonne V18 nucleon-nucleon potential plus a phenomenological three body force of Urbana type. Our results are compared thoroughly to those arising from several Skyrme and relativistic effective models. The values of the parameters characterizing the BHF equation of state of isospin asymmetric nuclear matter fall within the trends predicted by those models and are compatible with recent constraints coming from heavy ion collisions, giant monopole resonances or isobaric analog states. In particular we find a value of the slope parameter $L = 66.5$ MeV, compatible with recent experimental constraints from isospin diffusion, $L = 88 \pm 25$ MeV. The correlation between the neutron skin thickness of neutron-rich isotopes and the slope, L , and curvature, K_{sym} , parameters of the symmetry energy is studied. Our BHF results are in very good agreement with the correlations already predicted by other authors using non-relativistic and relativistic effective models. The correlations of these two parameters and the neutron skin thickness with the transition density from non-uniform to β -stable matter in neutron stars are also analyzed. Our results confirm that there is an inverse correlation between the neutron skin thickness and the transition density.

PACS numbers: 21.65.Cd; 21.65.Ef; 21.65.Mn

I. INTRODUCTION

A well-grounded understanding of the properties of isospin-rich nuclear matter is a necessary ingredient for the advancement of both nuclear physics and astrophysics. Isospin asymmetric nuclear matter is present in nuclei, especially in those far away from the stability line, and in astrophysical systems, particularly in neutron stars. A major scientific effort is being carried out at an international level to study experimentally the properties of asymmetric nuclear systems. Laboratory measurements, such as those running or planned to run in the existing or the next-generation, radioactive ion beam facilities at CSR (China), FAIR (Germany), RIKEN (Japan), SPIRAL2/GANIL (France) and the upcoming FRIB (USA), can probe the behavior of the symmetry energy close and above saturation density [1]. Moreover, the ^{208}Pb Radius Experiment (PREX), scheduled to run at JLab in early 2010, should provide a very accurate measurement of the neutron skin thickness in lead via parity violating electron scattering [2]. Astrophysical observations of compact objects are also a window into both the bulk and the microscopic properties of nuclear matter at extreme isospin asymmetries [3]. The symmetry energy determines to a large extent the composition of β -stable matter and therefore the structure and mass of a neutron star [4].

The empirical knowledge gathered from all these sources should be helpful in identifying the major issues arising when the isospin content of nuclear systems is altered. Reliable theoretical investigations of neutron-rich (and possibly proton-rich) systems are therefore called for. Phenomenological approaches, either relativistic or non-relativistic, are based on effective interactions that are frequently built in order to reproduce the properties of nuclei [5]. Since many of such interactions are built to describe systems close to the symmetric case, predictions at high asymmetries should be taken with care. A priori, the starting point of microscopic approaches appears to be safer: realistic nucleon-nucleon (NN) interactions reproduce the scattering and bound state properties of the free two-nucleon system and include naturally an isospin dependence [6]. The in-medium correlations are then built using many-body techniques that microscopically account for isospin asymmetry effects such as, for instance, the difference in the Pauli blocking factors of neutrons and protons in asymmetric systems [7].

In practical applications, phenomenological approaches can be significantly improved in the isospin asymmetric case by using, as input, microscopically based predictions. The

Skyrme interactions of the Lyon group [8, 9, 10] for instance, reproduce a neutron matter equation of state (EoS) based on microscopic variational calculations [11, 12] and are, therefore, able to predict reasonable properties for compact stars [13].

Even when these restrictions are taken into account, however, some of the properties of asymmetric nuclear matter appear to be rather unconstrained. In particular, the density dependence of the symmetry energy is still an important source of uncertainties. Different approaches predict similar asymmetry properties close to saturation, but strongly diverge for densities either above or below the saturation point. We shall try to give a quantitative prediction for the density dependences arising from a microscopic perspective. Let us note that the situation in symmetric nuclear matter is quite different: the saturation density, binding energy and incompressibility are relatively well settled from an empirical point of view. However, in microscopic calculations [14, 15, 16], the prediction of these saturation properties is strongly influenced by three-body forces (TBF), mainly concerning the determination of the saturation density that can be easily off by 40% in the absence of TBF. Other microscopic calculations using also realistic interactions have been recently reported in the framework of Dirac-Brueckner-Hartree-Fock [17, 18]

Values for the properties of asymmetric nuclear matter can be obtained from various analyses of experimental data, including isospin diffusion measurements [1], giant resonances [19], isobaric analog states [20] or meson production (pions [21], kaons [22]) in heavy ion collisions. Another important tool to determine empirically these properties are the existing correlations between different quantities in bulk matter and finite nuclei. The Typel-Brown correlation, for instance, is a linear relation between the density derivative of the neutron matter EoS at 0.1 fm^{-3} and the neutron skin thickness of ^{208}Pb that has been theoretically tested with different Skyrme parameter sets [23] and relativistic Hartree models [24]. Accurate measurements of neutron skin thicknesses, via future parity violating experiments [2] or by means of existing antiprotonic atoms data [25, 26], are thus helpful in determining the bulk properties of nuclear systems. Other linear correlations, such as those relating the ^{208}Pb skin thickness and the liquid-to-solid transition density in neutron stars [27], or power law correlations, such as the relation between the radius of a neutron star mass and the EoS [28], have also been observed. There is so much dispersion on the results of these correlations obtained with phenomenological approaches, that fully microscopic calculations, as the one performed in this paper, are needed.

In the present work, we compute the density dependence of the symmetry energy and physical quantities directly related with its slope and curvature obtained from a realistic interaction, namely the Argonne V18 [29] plus a TBF of the Urbana type, in the framework of the Brueckner–Hartree–Fock (BHF) approximation. After a brief discussion of the parametrization of the energy density and symmetry energy, and a short description of the BHF approach, we discuss and compare extensively our results with those obtained with several Skyrme forces and relativistic effective models. We pay particular attention to the trends established by these calculations and analyze different correlations arising from them. We conclude the discussion by summarizing the more important results.

II. ASYMMETRIC NUCLEAR MATTER

Assuming charge symmetry for nuclear forces, the energy per particle of asymmetric nuclear matter can be expanded on the isospin asymmetry parameter, $\beta = (N - Z)/(N + Z) = (\rho_n - \rho_p)/\rho$, around the values of symmetric ($\beta = 0$) nuclear matter, in terms of even powers of β as

$$\frac{E}{A}(\rho, \beta) = E_{SNM}(\rho) + S_2(\rho)\beta^2 + S_4(\rho)\beta^4 + \mathcal{O}(\beta^6), \quad (1)$$

where $E_{SNM}(\rho)$ is the energy per particle of symmetric matter, $S_2(\rho)$ is identified (excluding surface contributions [20, 26]) with the usual symmetry energy in the semi-empirical mass formula

$$S_2(\rho) = \frac{1}{2} \left. \frac{\partial^2 E/A}{\partial \beta^2} \right|_{\beta=0}, \quad (2)$$

and

$$S_4(\rho) = \frac{1}{24} \left. \frac{\partial^4 E/A}{\partial \beta^4} \right|_{\beta=0}. \quad (3)$$

It is well known, however, that the dominant dependence of the energy per particle of asymmetric nuclear matter on β , is essentially quadratic [7, 30, 31]. Therefore, contributions from S_4 and higher order terms can be neglected, and one can, in good approximation, estimate the symmetry energy simply from the two extreme cases of both pure neutron matter and symmetric nuclear matter according to

$$S_2(\rho) \sim \frac{E}{A}(\rho, 1) - \frac{E}{A}(\rho, 0). \quad (4)$$

In Fig. 1 we show the density dependences of the coefficients S_2 and S_4 obtained in our BHF calculation (left panel), together with the results predicted by the Skyrme force SLy230a

(middle panel) and the relativistic mean field model NL3 (right panel). For the three models, S_2 is an increasing function of the density [32] in the whole range of densities explored ($0 - 0.3 \text{ fm}^{-3}$). The rate at which S_2 increases is, however, substantially different for each of them: while NL3 predicts a steep, almost linear increase, SLy230a shows a substantial down bending above saturation. The BHF results appear to be somewhere in the middle of the two behaviors. Note that in the three cases, as expected, the coefficient S_4 is very small (below 0.5 MeV in the BHF case, and below 1 – 2 MeV in the case of the Skyrme force and the NL3 model) in the density region considered.

It is common to characterize the density dependence of the energy per particle of symmetric matter around the saturation density ρ_0 in terms of a few bulk parameters by expanding it in a Taylor series around ρ_0 ,

$$E_{SNM}(\rho) = E_0 + \frac{K_0}{2} \left(\frac{\rho - \rho_0}{3\rho_0} \right)^2 + \frac{Q_0}{6} \left(\frac{\rho - \rho_0}{3\rho_0} \right)^3 + \mathcal{O}(4) . \quad (5)$$

The coefficients denote, respectively, the energy per particle, the incompressibility coefficient and the third derivative of symmetric matter at saturation,

$$E_0 = E_{SNM}(\rho = \rho_0) , \quad K_0 = 9\rho_0^2 \frac{\partial^2 E_{SNM}(\rho)}{\partial \rho^2} \Big|_{\rho=\rho_0} , \quad Q_0 = 27\rho_0^3 \frac{\partial^3 E_{SNM}(\rho)}{\partial \rho^3} \Big|_{\rho=\rho_0} . \quad (6)$$

Similarly, the behaviour of the symmetry energy around saturation can be also characterized in terms of a few bulk parameters,

$$S_2(\rho) = E_{sym} + L \left(\frac{\rho - \rho_0}{3\rho_0} \right) + \frac{K_{sym}}{2} \left(\frac{\rho - \rho_0}{3\rho_0} \right)^2 + \frac{Q_{sym}}{6} \left(\frac{\rho - \rho_0}{3\rho_0} \right)^3 + \mathcal{O}(4) , \quad (7)$$

where E_{sym} is the value of the symmetry energy at saturation and the quantities L , K_{sym} and Q_{sym} are related to its slope, curvature and third derivative, respectively, at such density,

$$L = 3\rho_0 \frac{\partial S_2(\rho)}{\partial \rho} \Big|_{\rho=\rho_0} , \quad K_{sym} = 9\rho_0^2 \frac{\partial^2 S_2(\rho)}{\partial \rho^2} \Big|_{\rho=\rho_0} , \quad Q_{sym} = 27\rho_0^3 \frac{\partial^3 S_2(\rho)}{\partial \rho^3} \Big|_{\rho=\rho_0} . \quad (8)$$

Combining the expansions (1), (5) and (7), one can predict the existence of a saturation density, *i.e.*, a zero pressure condition, for a given asymmetry, and rewrite the energy per particle of asymmetric matter around the new saturation density $\rho_0(\beta) \sim \rho_0(1 - 3(L/K_0)\beta^2)$ in a form similar to Eq. (5),

$$\frac{E}{A}(\rho, \beta) = E_0(\beta) + \frac{K_0(\beta)}{2} \left(\frac{\rho - \rho_0(\beta)}{3\rho_0(\beta)} \right)^2 + \frac{Q_0(\beta)}{6} \left(\frac{\rho - \rho_0(\beta)}{3\rho_0(\beta)} \right)^3 + \mathcal{O}(4) , \quad (9)$$

where the coefficients $E_0(\beta)$, $K_0(\beta)$ and $Q_0(\beta)$ that characterize the energy per particle, the incompressibility coefficient and the third derivative at $\rho_0(\beta)$ for a given asymmetry β read up to second order

$$\begin{aligned} E_0(\beta) &= E_0 + E_{sym}\beta^2 + \mathcal{O}(4) \\ K_0(\beta) &= K_0 + \left(K_{sym} - 6L - \frac{Q_0}{K_0}L \right) \beta^2 + \mathcal{O}(4) \\ Q_0(\beta) &= Q_0 + \left(Q_{sym} - 9L\frac{Q_0}{K_0} \right) \beta^2 + \mathcal{O}(4) . \end{aligned} \quad (10)$$

Fig. 2 shows the saturation density (left panel), energy per particle (middle panel) and incompressibility (right panel) as a function of β^2 , up to a value of $\beta \sim 0.6$. For $\beta = 0$ one recovers the results of symmetric nuclear matter, then as β increases the saturation density, the binding energy and the incompressibility decrease. These behaviors are rather intuitive and a direct consequence of Eq. (10) and the specific values of E_{sym} , L , K_{sym} , K_0 and Q_0 at the saturation density of symmetric nuclear matter. Note that the BHF results are well reproduced by the quadratic expansion on β in the range of asymmetries considered.

In the following, before presenting our results, we shortly review the BHF approach of asymmetric nuclear matter and provide a few details on the Skyrme forces and the relativistic models considered.

A. The BHF approach of asymmetric matter

The BHF approach of asymmetric nuclear matter [7, 33] starts with the construction of all the G matrices describing the effective interaction between two nucleons in the presence of a surrounding medium. They are obtained by solving the well known Bethe–Goldstone equation

$$G_{\tau_1\tau_2;\tau_3\tau_4}(\omega) = V_{\tau_1\tau_2;\tau_3\tau_4} + \sum_{ij} V_{\tau_1\tau_2;\tau_i\tau_j} \frac{Q_{\tau_i\tau_j}}{\omega - \epsilon_i - \epsilon_j + i\eta} G_{\tau_i\tau_j;\tau_3\tau_4}(\omega) \quad (11)$$

where $\tau = n, p$ indicates the isospin projection of the two nucleons in the initial, intermediate and final states, V denotes the bare NN interaction, $Q_{\tau_i\tau_j}$ the Pauli operator that allows only intermediate states compatible with the Pauli principle, and ω , the so-called starting energy, corresponds to the sum of non-relativistic energies of the interacting nucleons. The single-particle energy ϵ_τ of a nucleon with momentum \vec{k} is given by

$$\epsilon_\tau(\vec{k}) = \frac{\hbar^2 k^2}{2m_\tau} + \text{Re}[U_\tau(\vec{k})] , \quad (12)$$

where the single-particle potential $U_\tau(\vec{k})$ represents the mean field “felt” by a nucleon due to its interaction with the other nucleons of the medium. In the BHF approximation, $U(\vec{k})$ is calculated through the “on-shell energy” G -matrix, and is given by

$$U_\tau(\vec{k}) = \sum_{\tau'} \sum_{|\vec{k}'| < k_{F_{\tau'}}} \langle \vec{k}\vec{k}' | G_{\tau\tau';\tau\tau'}(\omega = \epsilon_\tau(k) + \epsilon_{\tau'}(k')) | \vec{k}\vec{k}' \rangle_A \quad (13)$$

where the sum runs over all neutron and proton occupied states and where the matrix elements are properly antisymmetrized. We note here that the so-called continuous prescription has been adopted for the single-particle potential when solving the Bethe–Goldstone equation. As shown in Refs. [34, 35], the contribution to the energy per particle from three-hole line diagrams is minimized in this prescription. Once a self-consistent solution of Eqs. (11) and (13) is achieved, the energy per particle can be calculated as

$$\frac{E}{A}(\rho, \beta) = \frac{1}{A} \sum_{\tau} \sum_{|\vec{k}| < k_{F_{\tau}}} \left(\frac{\hbar^2 k^2}{2m_{\tau}} + \frac{1}{2} \text{Re}[U_{\tau}(\vec{k})] \right). \quad (14)$$

The BHF calculation carried out in this work uses the realistic Argonne V18 (Av18) [29] nucleon-nucleon interaction supplemented with a three-body force of Urbana type which for the use in BHF calculations was reduced to a two-body density dependent force by averaging over the third nucleon in the medium [36]. This three-body force contains two parameters that are fixed by requiring that the BHF calculation reproduces the energy and saturation density of symmetric nuclear matter (see Refs. [14, 15, 16] for a recent analysis of the use of three-body forces in nuclear and neutron matter). Note that the Av18 interaction contains terms that break explicitly isospin symmetry. Therefore, in principle, we should consider also odd powers of β in the expansion (1) in our Brueckner calculation. However, we have neglected such terms since, as shown by Mütter *et al.* in Ref. [6], the effects of isospin symmetry breaking in the symmetry energy are almost negligible (less than 0.5 MeV for a wide range of NN interactions).

B. Phenomenological Models

Effective nucleon-nucleon interactions of Skyrme type are very popular in nuclear structure calculations (see Ref. [5] for a recent review). The zero-range nature of this phenomenological NN interaction allows for a very efficient implementation of mean field calculations,

in both finite nuclei and extended nuclear matter where one can get simple analytical expressions. In fact, the main advantage of these forces comes from their analytical character, which make them very useful to get a physical insight into problems where the fully microscopic calculations are very difficult to implement. By construction, most of the Skyrme forces used in the literature are well behaved around the saturation density of nuclear matter and for moderate isospin asymmetries. However, not all Skyrme parameters are completely well determined through the fits of given sets of data and only certain combinations of the parameters are really empirically determined. This leads to a scenario where, for instance, different Skyrme forces produce similar equations of state for symmetric nuclear matter but very different results for neutron matter. Recently, an extensive and systematic study has tested the capabilities of almost 90 existing Skyrme parametrizations to provide good neutron-star properties. It was found that only twenty seven of these forces passed the restrictive tests imposed, the key property being the behavior of the symmetry energy with density [13]. In this work, we have only considered the forces that passed the tests imposed by Stone *et al.*, in Ref. [13]. Particular numerical results concerning some forces of the Lyon group, the SkI family (adjusted to isotopic shifts in the lead region) [37, 38] and the early SIII and SV [39] parametrizations will be discussed in Table I.

Regarding the relativistic effective approaches, we have considered two different types of models: (i) non-linear Walecka models (NLWM) with constant couplings, and (ii) density dependent hadronic models (DDH) with density dependent coupling constants. Within the first type, in particular, we have considered the models NL3 [40], TM1 [41] (which includes non-linear terms for the ω meson in order to soften the EOS at high densities), GM1 and GM3 [42], and FSU [43] (with non linear $\omega - \rho$ terms). For the second type we have considered the models TW [44], DD-ME1, DD-ME2 [45] and DDH δ [46]. The last one includes the δ -meson whose presence, as shown in Refs. [47] and [48], softens the symmetry energy at subsaturation densities and hardens it above saturation density. Finally, we have also considered the so-called quark-meson coupling model (QMC) [49]. In this model, nuclear matter is described as a system of non-overlapping MIT bags which interact through the exchange of scalar and vector mean fields. We have considered the parametrization used by Santos *et al.* in [50], where saturation properties of asymmetric nuclear within QMC were compared with other relativistic models. Although having a quite high compressibility, the isovector channel properties such as the symmetry energy and its derivatives with respect

to the density are within the intervals set by experimental measurements.

III. RESULTS

We start the analysis of our results by showing in Table I the bulk parameters characterizing the density dependence of the energy of symmetric matter and the symmetry energy around saturation density. Note that although all the models reasonably agree on their predictions for the energy per particle, symmetry energy, and density at saturation, they disagree in the remaining parameters, showing, in particular, significant discrepancies on the quantities Q_0 , L , K_{sym} and Q_{sym} , and on the parameter $K_\tau \equiv K_{sym} - 6L - (Q_0/K_0)L$ that characterizes the isospin dependence of the incompressibility coefficient [56, 57]. In the first three rows of the Table I we show our BHF results with and without three-body forces respectively. As already mentioned the TBF contains two parameters that are fixed in order to reproduce the saturation point of symmetric matter. In the Table we present results for two sets of such parameters: the original set of Ref. [36] (labelled TBFa), and a second one (labelled TBFb), in which the parameter associated with the two pion attractive term has been reduced by 10%, and the one associated with the phenomenological repulsive term been increased by 20% in order to get a smaller saturation density. As a consequence, the binding energy and the incompressibility coefficient at the new saturation point decrease a little bit (see Table I). The slightly different results obtained with TBFa or with TBFb give an insight on the importance of the more phenomenological component of our approach. For most of the properties associated to the EoS, the differences are relatively small, which suggests that the results that we obtain are rather robust. The comparison of the different quantities is strongly influenced by the fact that they are calculated at the saturation density of each approach. Note that the effects of TBF are more important on the iso-scalar properties as K_0 than on the properties associated to the density dependence of the symmetry energy. All the BHF results shown in the different figures contain the effects of TBF and have been obtained with the original set of parameters of Ref. [36].

Recent results from isospin diffusion (ID) predict values of $L = 88 \pm 25$ MeV and $K_\tau = -500 \pm 50$ MeV [1, 51]. The latter is in agreement with the value of $K_\tau = -550 \pm 100$ MeV predicted by the independent measurement of the isotopic dependence of the giant monopole resonance (GMR) in Sn isotopes [19, 52]. Similar values of L have also been

obtained by using experimental double ratios of proton and neutron spectra together with improved quantum molecular dynamics calculations [53]. While our Brueckner calculation leads to a value of $L = 66.5$ MeV, compatible with the data from isospin diffusion, our prediction of $K_\tau = -334.7$ MeV is far from the lower bound $K_\tau = -450$ MeV imposed by experiments. However, one has to be cautious when interpreting our parameter K_τ , defined in asymmetric nuclear matter, with the experimental data which, as pointed out by Blaizot and Grammaticos [54], may be related to the isospin-dependent part of the surface properties of finite nuclei, especially the surface symmetry energy. Note that the effect of TBF on these two parameters is only of about 5 – 10%. Furthermore, only the Skyrme force SV and the relativistic models TM1, GM1 and QMC predict values of L and K_τ both compatible with experimental constrains, although their predictions for K_0 are much larger than the value of $K_0 = 240 \pm 20$ MeV, supported nowadays by experimental data [55]. A close inspection to Table I shows, in fact, that none of the models considered predicts values of K_0, L and K_τ simultaneously consistent with the present experimental data. In fact, as pointed out recently by several authors [56, 57, 58, 59], it is difficult to determine the experimental value of K_τ accurately, since no single theoretical model is able to describe correctly the recent measurements of the isotopic dependence of GMR in Sn isotopes and, simultaneously, the GMR energies of a variety of nuclei. That suggests, as discussed by Piekarewicz and Centelles in Ref. [56], that the value of $K_\tau = -550 \pm 100$ MeV [19, 52] may suffer from the same ambiguities already encountered in earlier attempts to extract the incompressibility coefficient of infinite nuclear matter from finite-nuclei extrapolations. Concerning the third density derivative of the symmetry energy Q_{sym} , for which there is not, at present, any experimental constraint, the microscopic prediction is large and negative which is in contrast with most of the effective models (except TM1) that give a large variety of positive values.

In Fig. 3, we show the density dependence of $S_2(\rho)$ (left panel) for our BHF calculations and some representative Skyrme forces and relativistic models. In general, there is a good agreement between the microscopic BHF calculation and the Skyrme models considered in the whole density range explored. The relativistic models considered also agree with the BHF calculation at low densities, but deviations are found for TM1 and NL3 above saturation densities. A better insight of the density dependence of $S_2(\rho)$ can be obtained by looking at the density dependence of the slope parameter L . The results for the same models are

plotted in the right panel of the figure. Note that even the models that apparently show a similar behaviour of the symmetry energy with density, as for instance the relativistic TW model and our BHF calculation, predict a different density dependence of L . In general the relativistic models predict a stiffer dependence of the symmetry energy, reflected in larger values of L than those produced in BHF. The Skyrme models shown in the figure, produce smaller values of L . These are selected models whose density behaviour of the symmetry energy has been tested [13].

We show in Fig. 4 the correlations between L and K_{sym} (left panel) and L and K_τ (right panel), already considered in the literature for the case of effective forces [20, 57]. Note that the BHF results for L are located inside the region delimited by the isospin diffusion data constraints, and that they adjust reasonably well to these correlations. There is no direct empirical information on the K_{sym} parameter. However, as pointed out recently by Chen *et al.* in Ref. [57], whenever accurate experimental information becomes available for L , these correlations could be exploited to obtain theoretical estimates for K_{sym} and K_τ .

It has been shown by Brown and Typel [23, 24], and confirmed latter by other authors [3, 26, 27, 43, 51, 60, 61], that the neutron skin thickness, $\delta R = \sqrt{\langle r_n^2 \rangle} - \sqrt{\langle r_p^2 \rangle}$, calculated in mean field models with either non-relativistic or relativistic effective interactions is very sensitive to the density dependence of the nuclear symmetry energy, and, in particular, to the slope parameter L at the normal nuclear saturation density. Using our Brueckner approach and the several Skyrme forces and relativistic models considered we have made an estimation the neutron skin thickness of ^{208}Pb and ^{132}Sn and we have studied its correlation with the parameters L and K_{sym} . However, a fully self-consistent finite nuclei calculation based on the BHF approach is too difficult to implement, therefore, following the suggestion of Steiner *et al.* in Ref. [3] we have estimated δR to lowest order in the diffuseness corrections as $\delta R \sim \sqrt{\frac{3}{5}}t$, being t the thickness of semi-infinite asymmetric nuclear matter,

$$t = \frac{\beta_c}{\rho_0(\beta_c)(1 - \beta_c^2)} \frac{E_s}{4\pi r_0^2} \frac{\int_0^{\rho_0(\beta_c)} \rho^{1/2} [E_{sym}/S_2(\rho) - 1] [E_{SNM}(\rho) - E_0]^{-1/2} d\rho}{\int_0^{\rho_0(\beta_c)} \rho^{1/2} [E_{SNM}(\rho) - E_0]^{1/2} d\rho}. \quad (15)$$

In the above expression E_s is the surface energy taken from the semi-empirical mass formula equal to 17.23 MeV, r_0 is obtained from the normalization condition $(4\pi r_0^3/3)(0.16) = 1$, and β_c is the isospin asymmetry in the center of the nucleus. We have checked from Thomas-Fermi calculations that the value of β_c is about 1/2 of the total isospin asymmetry of the nucleus β if Coulomb effects are not considered as in the present case. Therefore, we have

taken $\beta_c = \beta/2$. Although we can perform finite nuclei calculations with the Skyrme and relativistic effective models, we have also used Eq. (15) with these models for consistency reasons with the BHF approach. We have checked that in the case of the Skyrme forces the accuracy of the results obtained by using Eq. (15) with respect to a Hartree–Fock calculation is about 15 – 25%.

In Fig. 5 we show the correlation between δR for ^{208}Pb (upper panels) and ^{132}Sn (lower panels) with the parameters L (left panels) and K_{sym} (right panels). It can be seen, as has already been shown by other authors, that both the Skyrme forces and the relativistic models predict values of δR that exhibit a tight linear correlation with L . Note that the microscopic Brueckner calculation is in excellent agreement with this correlation. Since K_{sym} is linearly correlated with L , it is, therefore, not surprising that δR presents also an almost linear correlation with K_{sym} , although it is less strong than its correlation with L , and shows a slight irregular behaviour. The linear increase of δR with L is not surprising since, as discussed in Refs. [3, 26, 27, 43, 51, 60, 61], the thickness of the neutron skin in heavy nuclei is determined by the pressure difference between neutrons and protons, which is proportional to the parameter L , $P(\rho_0, \beta) \sim L\rho_0\beta^2/3$ [20]. This can be seen for instance in Fig. 6, where we show the pressure of asymmetric nuclear matter evaluated at normal saturation density ρ_0 for the isospin asymmetries of ^{208}Pb ($\beta = 44/208$) and ^{132}Sn ($\beta = 32/132$). Note that, since the BHF calculation predicts larger values for ρ_0 than the other approaches (see Table I), its result appears in both cases, ^{208}Pb and ^{132}Sn , a bit out of the trends marked by the other models.

Another sensitive quantity to the symmetry energy is the transition density ρ_t from non-uniform to uniform β -stable matter which may be estimated from the crossing of the β -equilibrium equation of state with the thermodynamical spinodal instability line [48, 62, 63, 64, 65, 66]. As it has been shown in Ref. [65] the predictions for the transition density from the thermodynamical spinodal are $\sim 15\%$ larger than the value obtained from a Thomas–Fermi calculation of the pasta phase. Therefore, we may expect that our estimation of the transition density from the thermodynamical spinodal will define an upper bound to the true transition density [67]. We display in Fig. 7 ρ_t as a function of the parameters L and K_{sym} for our BHF calculation together with the predictions of the several Skyrme forces and relativistic models. It is clear from the figure that ρ_t is sensitive to the slope and curvature parameters L and K_{sym} of the symmetry energy, decreasing almost linearly with increasing

L and K_{sym} in agreement with recent results [66, 68]. Using the experimental constraint on L from isospin diffusion, we estimate the transition density to be between 0.063 fm^{-3} and 0.083 fm^{-3} . This range is in reasonable agreement with the the value of $\rho_t \approx 0.08 \text{ fm}^{-3}$ often used in the literature. Recently, Xu *et al.*, [66] have obtained a different range for the transition density, namely, from 0.04 to 0.065 fm^{-3} using 51 Skyrme interactions. These authors argue that their results are smaller than 0.08 fm^{-3} because their approach is exact and no parabolic approximation is assumed for the isospin dependence of the nuclear force. However, we note that in the present work the parabolic assumption has only been considered in the BHF calculation whereas all the other results are exact and the obtained range of transition densities is in all cases the one indicated above.

Finally, we show in Fig. 8 the transition density ρ_t from non-uniform to β -stable matter as a function of the neutron skin thickness in ^{208}Pb (left panel) and ^{132}Sn for our Brueckner calculation and the different Skyrme forces and relativistic models. The figure shows, as already pointed out by Horowitz and Piekarewicz [27] that there is an inverse correlation between the neutron skin thickness and ρ_t . In [27] a NLWM with non-linear $\omega - \rho$ terms was used and the transition density was obtained with an RPA approach. We confirm the same trend for a larger set of nuclear models. Note that, again, our microscopic Brueckner results are in very good agreement with this correlation. As pointed out in Ref. [27], these results suggest that an accurate measurement of the neutron radius in heavy nuclei like ^{208}Pb or ^{132}Sn is very important since it can provide considerable and valuable information on the thickness and other properties of neutron star's crust.

IV. SUMMARY

We have studied the density dependence of the symmetry energy within the microscopic Brueckner-Hartree-Fock approach using the realistic AV18 potential plus a three-body force of Urbana type. Our results have been compared with those obtained with several Skyrme forces and relativistic effective models. We have found a value of the slope parameter $L = 66.5 \text{ MeV}$, compatible with recent experimental constraints from isospin diffusion, $L = 88 \pm 25 \text{ MeV}$. We have studied the correlation between the neutron skin thickness of neutron-rich isotopes and L and K_{sym} . We have found that the BHF results are in very good agreement with the correlations already predicted by other authors using non-relativistic and

relativistic effective models. This agreement suggests that these correlations are not only due to the mean-field nature of these approaches. Microscopic calculations, as the one performed here, also provide a meaningful description of the isoscalar and isovector properties of the EoS and complement the already gathered knowledge on the bulk parameters of nuclear matter. We have also analyzed the correlations of L , K_{sym} and the neutron skin thickness with the transition density ρ_t from non-uniform to β -stable matter in neutron stars. Using the experimental constraint on L from isospin diffusion, we have estimated the value of ρ_t to be between 0.063 fm^{-3} and 0.083 fm^{-3} , a range in reasonable agreement with the value of $\rho_t \approx 0.08 \text{ fm}^{-3}$ often used in the literature. Finally, we have confirmed for a large set of nuclear models that there is an inverse correlation between the neutron skin thickness and the transition density ρ_t , a trend pointed out first by Horowitz and Piekarewicz in Ref. [27].

Acknowledgments

We are very grateful to Xavier Viñas, Mario Centelles, Jorge Piekarewicz and Xavier Roca-Maza for useful and stimulating discussions and comments. This work was partially supported by FEDER/FCT (Portugal) under the project CERN/FP/83505/2008, the Consolider Ingenio 2010 Programme CPAN CSD2007-00042 and grants No. FIS2008-01661 from MEC and FEDER and No. 2005SGR-00343 from Generalitat de Catalunya, the NSF (US) under Grants PHYS-0555893 and PHYS-0800026 and the STFC grant ST/F012012, the Project of Knowledge Innovation Program (PKIP) of Chinese Academy of Sciences, Grant No. KJCX2.YW.W10, and COMPSTAR, an ESF Research Networking Programme.

-
- [1] B. A. Li, L. W. Chen and C. M. Ko, Phys. Rep. **464**, 113 (2008).
 - [2] C. J. Horowitz, S. J. Pollock, P. A. Souder and R. Michaels, Phys. Rev. C **63**, 025501 (2001).
 - [3] A. W. Steiner, M. Prakash, J. Lattimer and P. J. Ellis, Phys. Rep. **411**, 325 (2005).
 - [4] H.-J. Schulze, A. Polls, A. Ramos, and I. Vidaña, Phys. Rev. C **73**, 058801 (2006).
 - [5] J. R. Stone and P.-G. Reinhard, Prog. Part. Nucl. Phys. **58**, 587 (2007).
 - [6] H. Müther, A. Polls and R. Machleidt, Phys. Lett. B **445**, 259 (1999).
 - [7] I. Bombaci and U. Lombardo, Phys. Rev. C **44**, 1892 (1991).

- [8] E. Chabanat, P. Bonche, P. Haensel, J. Meyer and R. Schaeffer. Nucl. Phys. A **635**, 231 (1998).
- [9] E. Chabanat, Ph. D. Thesis, Lyon, 1995.
- [10] E. Chabanat, P. Bonche, P. Haensel, J. Meyer and R. Schaeffer. Nucl. Phys. A **627**, 710 (1997).
- [11] A. Akmal, V.R. Pandharipande, and D.G. Ravenhall, Phys. Rev. C **58**, 1804 (1998).
- [12] H. Heiselberg and M. Hjorth-Jensen, Phys. Rep. **328**, 237 (2000).
- [13] J. R. Stone, J. C. Miller, R. Koncewicz, P. D. Stevenson and M. R. Strayer, Phys. Rev. C **68**, 034324 (2003).
- [14] X. R. Zhou, G F. Burgio, U. Lombardo, H.-J. Schulze and W. Zuo, Phys. Rev. C **69**, 018801 (2004).
- [15] Z. H. Li, U. Lombardo, H.-J. Schulze and W. Zuo, Phys. Rev. C **77**, 034316 (2008).
- [16] Z. H. Li and H.-J. Schulze, Phys. Rev. C **78**, 028801 (2008).
- [17] F. Sammarruca and P. Liu, Phys. Rev. C **79**, 057301 (2009).
- [18] P. Gögelein, E.N.E. van Dalen, Kh. Gad, Kh. S.A. Hassaneen, and H. Müther, Phys. Rev. C **79**, 024308 (2009).
- [19] U. Garg *et al.*, Nucl. Phys. A **788**, 36 (2007).
- [20] P. Danielewicz and J. Lee, Nucl. Phys. A **818**, 36 (2009).
- [21] B. A. Li, G.-C. Yang and W. Zuo, Phys. Rev. C **71**, 014608 (2005).
- [22] C. Fuchs, Prog. Part. Nucl. Phys. **56**, 1 (2006).
- [23] B. A. Brown, Phys. Rev. Lett. **85**, 5296 (2000).
- [24] S. Typel and B. A. Brown, Phys. Rev. C **64**, 027302 (2001).
- [25] B. A. Brown, G. Shen, G. C. Hillhouse, J. Meng and A. Trzcinska, Phys. Rev. C **76**, 034305 (2007).
- [26] M. Centelles, X. Roca-Maza, X. Viñas and M. Warda, Phys. Rev. Lett. **102**, 122502 (2009).
- [27] C. J. Horowitz and J. Piekarewicz, Phys. Rev. Lett. **86**, 5647 (2001).
- [28] J. M. Lattimer and M. Prakash, Astrophys. J. **550**, 426 (2001).
- [29] R. B. Wiringa, V. G. J. Stoks and R. Schiavilla, Phys. Rev. C **51**, 38 (1995).
- [30] C.-H. Lee, T. T. S. Kuo, G. Q. Li and G. E. Brown, Phys. Rev. C **57**, 3488 (1997).
- [31] T. Frick, H. Müther, A. Rios, A. Polls and A. Ramos, Phys. Rev. C **71**, 014313 (2005).
- [32] L. Engvik, M. Hjorth-Jensen, R. Machleidt, H. Müther, A. Polls, Nucl. Phys. A **627** 85 (1997).

- [33] W. Zuo, I. Bombaci and U. Lombardo, Phys. Rev. C **60**, 024605 (1999).
- [34] H. Q. Song, M. Baldo, G. Giansiracusa and U. Lombardo, Phys. Rev. Lett. **81**, 1584 (1998).
- [35] M. Baldo, G. Giansiracusa, U. Lombardo and H. Q. Song, Phys. Lett. B **473**, 1 (2000).
- [36] M. Baldo and L. Ferreira, Phys. Rev. C **59**, 682 (1999).
- [37] P.-G. Reinhard and H. Flocard, Nucl. Phys. A **584**, 467 (1995).
- [38] W. Nazarewicz, J. Dobaczewski, T. R. Werner, J. A. Maruhn, P.-G. Reinhard, K. Rutz, C. R. Chinn, A. S. Umar and M. R. Strayer, Phys. Rev. C **53**, 740 (1996).
- [39] M. Beiner, H. Flocard, N. Van Giai and P. Quentin, Nucl. Phys. A **238**, 29 (1975)
- [40] G. A. Lalazissis, J. Köning and P. Ring, Phys. Rev. C **55** 540 (1997).
- [41] K. Sumiyoshi, H. Kuwabara, H. Toki, Nucl. Phys. A **581**, 725 (1995).
- [42] N. K. Glendenning and S. A. Moszkowski, Phys. Rev Lett. **67**, 2414 (1991).
- [43] B. G. Todd–Rutel and J. Piekarewicz, Phys. Rev. Lett. **95**, 122501 (2005).
- [44] S. Typel and H. H. Wolter, Nucl. Phys. A **656**, 331 (1999).
- [45] T. Niksic, D. Vretenar, P. Finelli and P. Ring, Phys. Rev. C **66**, 024306 (2002); G. A. Lalazissis, T. Niksic, D. Vretenar and P. Ring, Phys. Rev. C **72**, 024312 (2005).
- [46] T. Gaitanos, M. Di Toro, S. Typel, V. Baran, C. Fuchs, V. Greco and H. H. Wolter, Nucl. Phys. **A732**, 24 (2004).
- [47] B. Liu, V. Greco, V. Baran, M. Colonna and M. Di Toro, Phys. Rev. C **65**, 045201 (2002).
- [48] C. Ducoin, C. Providência, A. M. Santos, L. Brito and Ph. Chomaz, Phys. Rev. C **78**, 055801 (2008).
- [49] P. A. M. Guichon, Phys. Lett. **B 200**, 235 (1988); K. Saito and A.W. Thomas, Phys. Lett. **B 327**, 9 (1994); K. Tsushima, K. Saito, A.W. Thomas and S.V. Wright, Phys. Lett. B **429**, 239 (1998).
- [50] A. M. Santos, C. Providência, and P. K. Panda, Phys. Rev. C **79**, 045805 (2009).
- [51] L. W. Chen, C. M. Ko and B. A. Li, Phys. Rev. Lett. **94**, 032701 (2005); Phys. Rev. C **72**, 064309 (2005).
- [52] T. Li *et al.*, Phys. Rev. Lett. **99**, 162503 (2007).
- [53] M. B. Tsang, Y. Zhang, P. Danielewicz, M. Famiano, Z. Li, W. G. Lynch and A. W. Steiner, Phys. Rev. Lett. **102**, 122701 (2009).
- [54] J. P. Blaizot and B. Grammaticos, Nucl. Phys. A **355**, 115 (1981).
- [55] D. H. Youngblood, H. L. Clark and Y.-W. Lui, Phys. Rev. Lett. **82**, 691 (1999).

- [56] J. Piekarewicz and M. Centelles, *Phys. Rev. C* **79**, 054311 (2009).
- [57] L. W. Chen, B. J. Cai, C. M. Ko, B. A. Li, C. Shen and J. Xu, *Phys. Rev. C* **80**, 014322 (2009).
- [58] J. Piekarewicz, *Phys. Rev. C* **76**, 031301(R) (2007).
- [59] H. Sagawa, S. Yoshida, G. M. Zeng, J. Z. Gu and X. Z. Zhang, *Phys. Rev. C* **76**, 034327 (2007).
- [60] R. J. Furnstahl, *Nuc. Phys. A* **706**, 85 (2002).
- [61] A. E. L. Dieperink, Y. Dewulf, D. Van Neck, M. Waroquier and V. Rodin, *Phys. Rev. C* **68**, 064307 (2003).
- [62] S. S. Avancini, L. Brito, Ph. Chomaz, D. P. Menezes, C. Providência, *Phys. Rev. C* **74**, 024317, (2006).
- [63] I. Vidaña and A. Polls, *Phys. Lett. B* **666**, 232 (2008).
- [64] S.S. Avancini, D.P. Menezes, M.D. Alloy, J.R. Marinelli, M.M.W. Moraes and C. Providência, *Phys. Rev. C* **78**, 015802 (2008).
- [65] S.S. Avancini, L. P. Brito, J.R. Marinelli, D.P. Menezes, M.M.W. Moraes, C. Providência and A. M. Santos, *Phys. Rev. C* **79**, 035804 (2009).
- [66] J. Xu, L.W. Chen, B.A. Li and H.R. Ma, *Astrophys. J.* 697, 1549 (2009)
- [67] C. J. Pethick, D. G. Ravenhall and C. P. Lorenz, *Nucl. Phys. A* **584**, 675 (1995); F. Douchin and P. Haensel, *Phys. Lett. B* **485**, 107 (2000).
- [68] K. Oyamatsu and K. Iida, *Phys. Rev. C* **75**, 015801 (2007).

Model	ρ_0	E_0	K_0	Q_0	E_{sym}	L	K_{sym}	Q_{sym}	K_τ	Ref.
BHF (with TBFa)	0.187	-15.23	195.5	-280.9	34.3	66.5	-31.3	-112.8	-334.7	
BHF (with TBFb)	0.176	-14.62	185.9	-224.9	33.6	66.9	-23.4	-162.8	-343.8	
BHF (without TBF)	0.240	-17.30	213.6	-225.1	35.8	63.1	-27.8	-159.8	-339.6	
SLy4	0.159	-15.97	229.8	-362.9	31.8	45.3	-119.8	520.8	-320.4	[8]
SLy10	0.155	-15.90	229.7	-358.3	32.1	39.2	-142.4	590.9	-316.7	[9]
SLy230a	0.160	-15.98	229.9	-364.2	31.8	43.9	-98.4	602.8	-292.7	[10]
SkI4	0.162	-16.15	250.3	-335.7	29.6	59.9	-43.4	358.8	-322.5	[37]
SkI5	0.156	-15.84	255.6	-301.7	36.4	128.9	159.8	11.2	-461.6	[37]
SkI6	0.159	-15.88	248.2	-326.7	34.4	82.1	-0.9	332.3	-385.8	[38]
SIII	0.145	-15.85	353.9	101.3	28.1	10.1	-392.3	130.2	-456.0	[39]
SV	0.155	-16.04	305.3	-175.5	32.9	96.5	24.1	48.0	-499.4	[39]
NL3	0.148	-16.24	271.6	203.1	37.4	118.5	100.9	181.2	-698.4	[40]
TM1	0.145	-16.32	281.0	-285.2	36.8	110.8	33.6	-66.4	-518.7	[41]
GM1	0.153	-16.32	299.2	-216.5	32.4	93.9	17.9	25.1	-477.5	[42]
GM3	0.153	-16.32	239.7	-512.9	32.4	89.7	-6.5	55.8	-352.7	[42]
FSU	0.148	-16.30	230.0	-523.4	32.6	60.5	-51.3	424.1	-276.6	[43]
TW	0.153	-16.25	240.1	-540.1	32.7	55.3	-124.7	535.2	-332.1	[44]
DDME1	0.152	-16.23	243.7	332.8	33.1	55.6	-100.8	703.8	-508.1	[45]
DDME2	0.152	-16.14	250.8	478.1	32.3	51.4	-86.6	773.9	-493.8	[45]
DDH δ	0.153	-16.25	240.2	-539.7	25.1	44.0	44.9	928.3	-120.2	[46]
QMC	0.150	-15.70	291.0	-387.5	33.7	93.5	-10.0	28.0	-446.4	[49]

TABLE I: Bulk parameters characterizing the density dependence of the energy of symmetric matter and the symmetry energy around saturation density for the BHF calculation with and without TBF and several Skyrme forces and relativistic models. All the quantities are in MeV, with the exception of ρ_0 given in fm^{-3} .

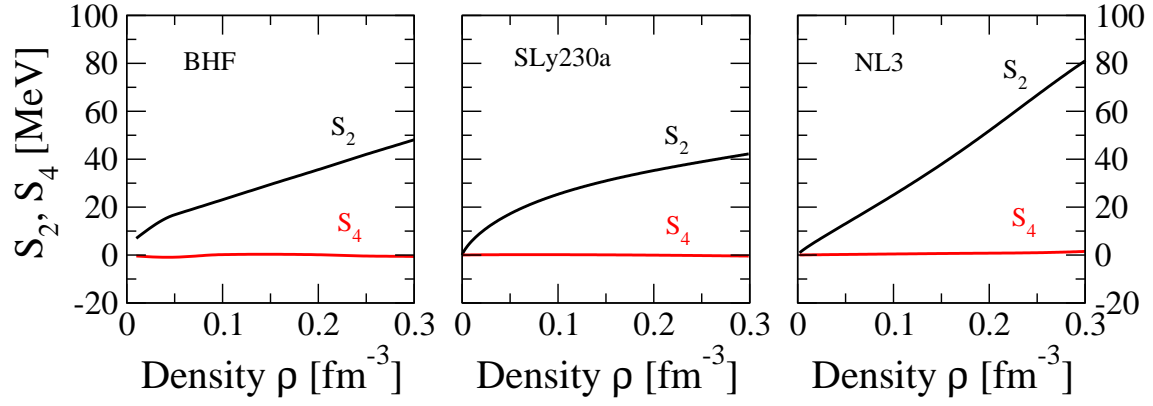


FIG. 1: (Color online) Density dependence of the symmetry energy coefficients S_2 and S_4 . Results for the BHF calculation, the Skyrme force SLy230a and the relativistic model NL3 are shown in the left, middle and right panels, respectively.

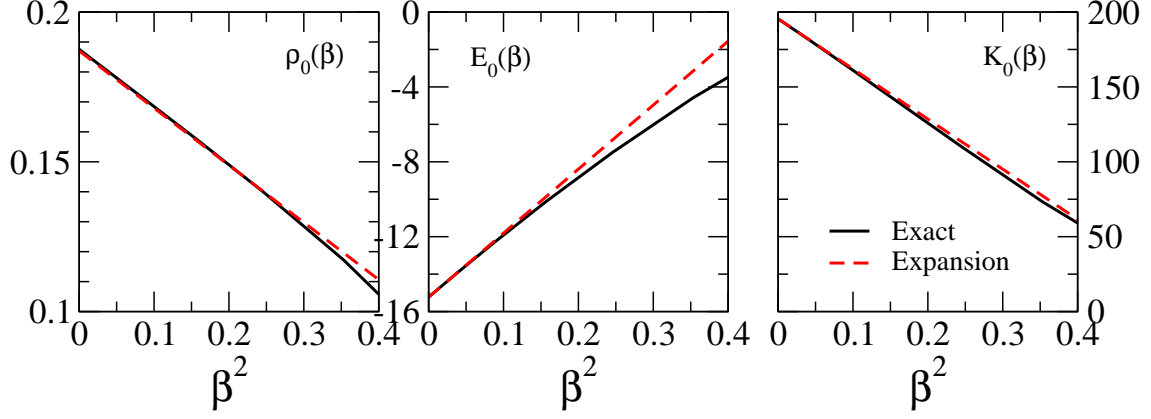


FIG. 2: (Color online) Isospin asymmetry dependence of the density (left panel), energy per particle (middle panel) and incompressibility coefficient (right panel) at the saturation point of asymmetric nuclear matter. Solid lines show the results of the exact BHF calculation whereas dashed lines indicate the results of the expansion of Eq. (10). Units of $E_0(\beta)$ and $K_0(\beta)$ are given in MeV whereas $\rho_0(\beta)$ is given in fm^{-3} .

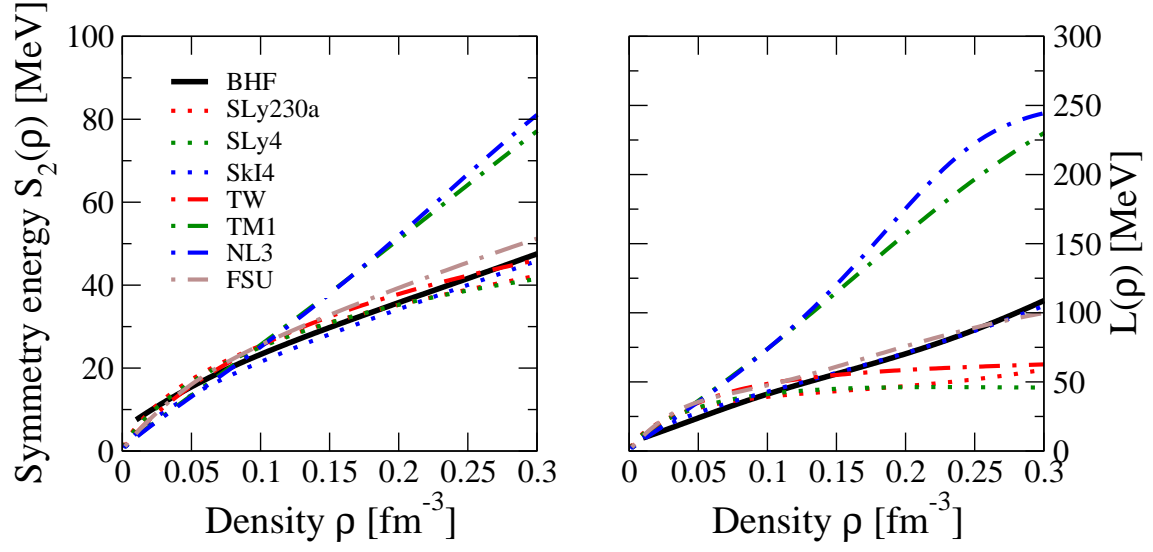


FIG. 3: (Color online) Density dependence of the symmetry energy (left panel) and L (right panel) for the BHF calculation and some of the considered Skyrme forces and relativistic models.

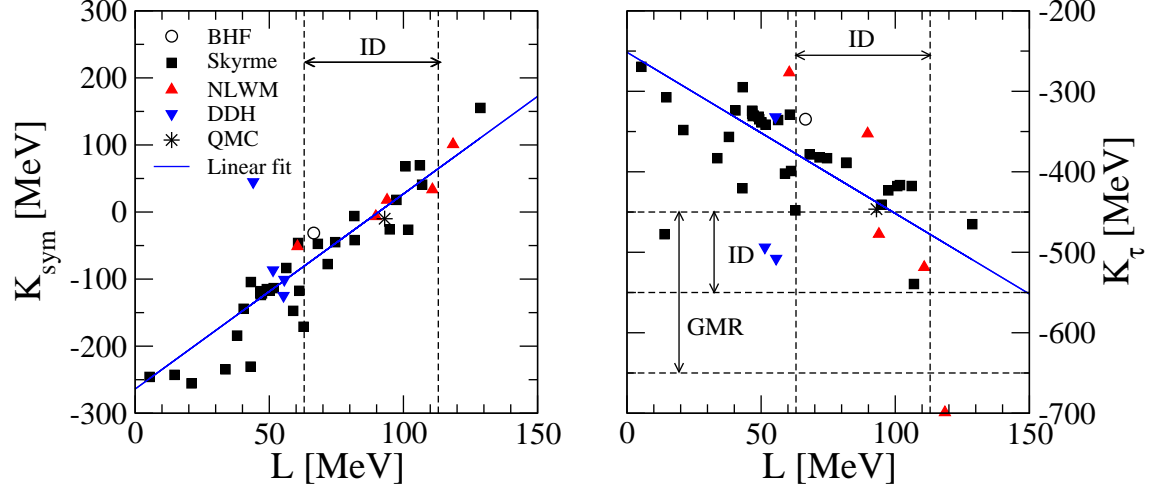


FIG. 4: (Color online) Correlation of K_{sym} (left panel) and K_{τ} (right panel) with L . The vertical and horizontal dashed lines on the right panel denote the constraints on L and K_{τ} from isospin diffusion (ID) [1, 51] and on K_{τ} from measurements of the isotopic dependence of giant monopolar resonances (GMR) in Sn isotopes [19, 52].

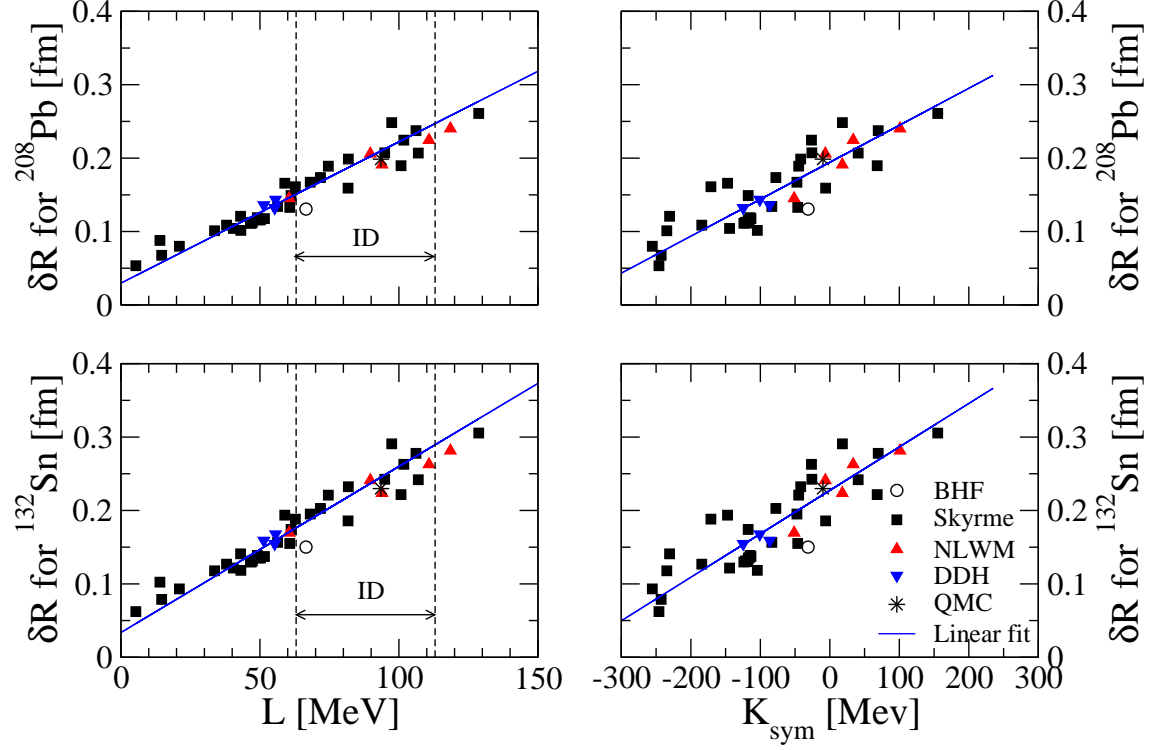


FIG. 5: (Color online) Neutron skin thickness for ^{208}Pb (upper panels) and ^{132}Sn (lower panels) versus L (left panels) and K_{sym} (right panels). The vertical dashed lines on the left panels denote the constraints on L from isospin diffusion (ID) [1, 51].

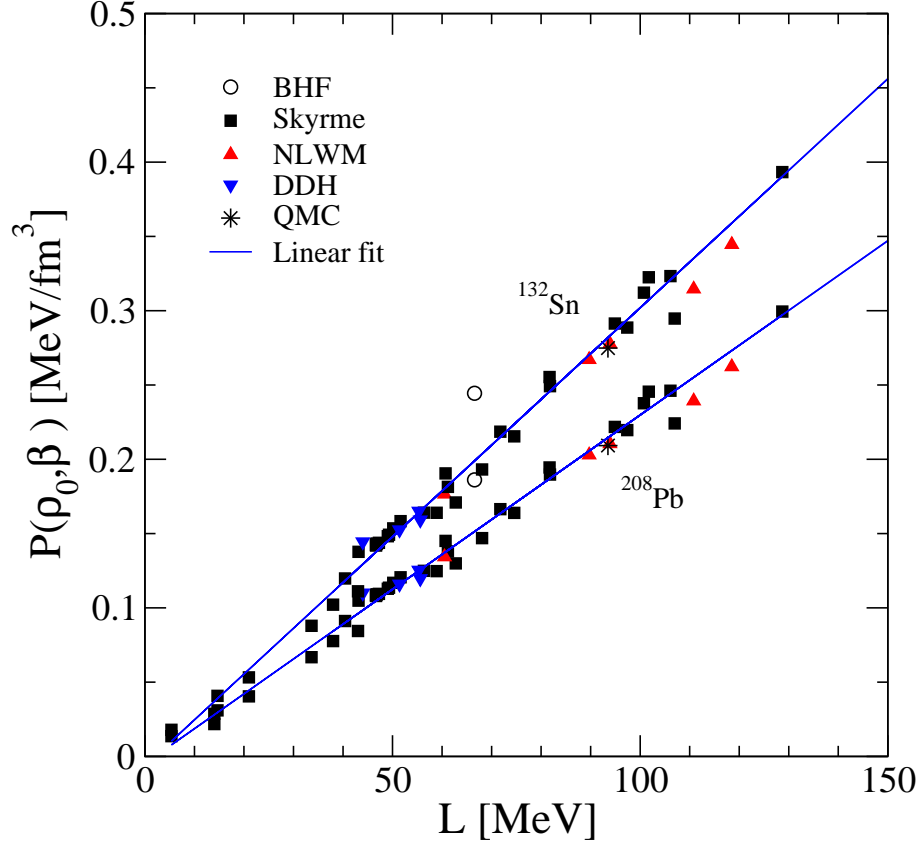


FIG. 6: (Color online) Pressure of asymmetric nuclear matter at ρ_0 as a function of L for the isospin asymmetries of ^{208}Pb ($\beta = 44/208$) and ^{132}Sn ($\beta = 32/132$).

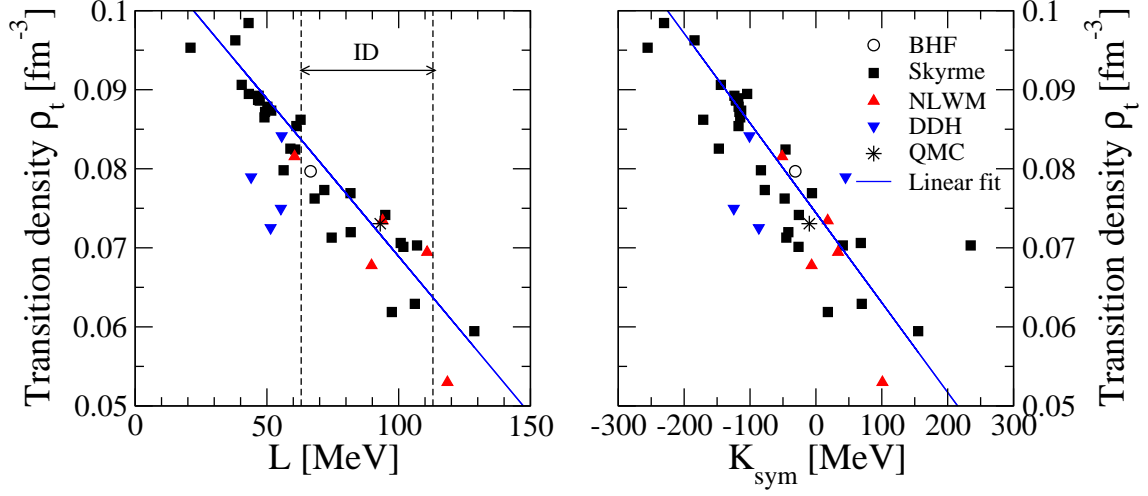


FIG. 7: (Color online) Transition density from non-uniform to uniform β -stable matter as a function of L (left panel) and K_{sym} (right panel). The vertical dashed lines on the left panel denote the constraints on L from isospin diffusion (ID) [1, 51].

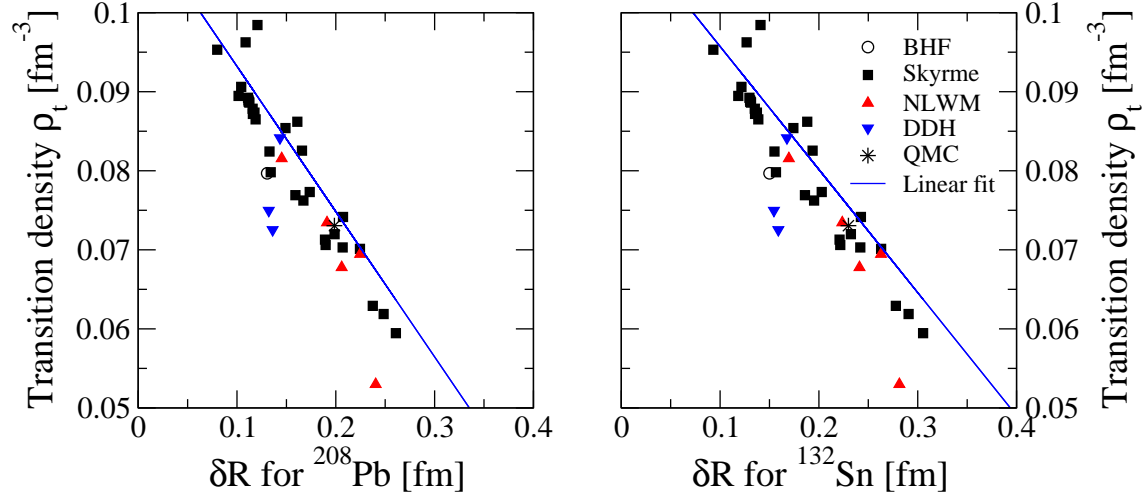


FIG. 8: (Color online) Transition density from non-uniform to uniform β -stable matter versus the neutron skin thickness for ^{208}Pb (left panel) and ^{132}Sn (right panel).